Preparation of platinum core–polyaryl ether aminediacetic acid dendrimer shell nanocomposite for catalytic hydrogenation of phenyl aldehydes

Yukou Du[a], Wei Zhang[a], Xiaomei Wang[b], and Ping Yang[a],*

[a]College of Chemistry and Chemical Engineering, Soochow University, Suzhou, 215006, P.R. China
[b]College of Materials Science and Engineering, Soochow University, Suzhou, 215021, P.R. China

Polyaryl ether aminediacetic acid dendrons (Gn-NA) were synthesized and used as stabilizer for preparing Pt nanoparticles. The resulting Pt nanoparticles have mean particle size from 2 to 5 nm depending on dendrimer generations and the molar ratio of metal/dendrimer. Most of the surface of the as-prepared platinum clusters, on which the dendrimers attached on the platinum core via the interactions between carboxyl groups and surface Pt atoms, remains unpassivated. Turnover frequencies for the hydrogenation of phenyl aldehydes to phenyl alcohols change from 91 to 25 depending on the dendrimer generation and substrates under an atmospheric pressure of H_2. The Pt particles capped with Gn-NA are stable during the catalytic hydrogenation process and can be easily recovered and reused. The result suggests the effectiveness of polyaryl ether aminediacetic acid dendrimer as a stabilizer for the preparation of Pt nanoparticle catalysts.

KEY WORDS: dendrimer; platinum nanoparticles; phenyl aldehydes; catalytic hydrogenation.

1. Introduction

Dendrimer-encapsulated metal nanoparticles and metal-nanoparticle cored dendrimers have attracted increasing interest in recent years since their potential use in homogeneous catalysis [1–4]. Several research groups have demonstrated that transitional metal nanoparticles encapsulated inside dendrimers in a variety of architectures [5–9]. The dendrimer-encapsulated metal nanoparticles showed to be efficient catalysts for Heck reaction and hydrogenation [10–17]. In a recent paper, the group of Fox has described a palladium-nanoparticle cored dendrimers for catalytic applications of Heck and Suzuki reaction [14]. Reduction of K_2PdCl_4 in the presence of Fréchet-type dendritic polyaryl ether disulfide of generation three resulted in the formation of palladium-nanoparticle-cored dendrimers (Pd-G-3). Nearly 90% of the Pd-G-3 surface remains unpassivated and available for catalysis. The coupling reactions catalyzed by Pd-G-3 can be performed under homogeneous or heterogeneous conditions with high TON and TOF. However, Pd-G-3 cannot be employed as catalyst for hydrogenation reactions since the carbon–sulphur bonds in Pd-G-3 were broken under the hydrogenation conditions, leading to the precipitation of the metal. In order to get stable metal-nanoparticle and maintain the surface of the metal particle unpassivated for hydroge-

nation reactions, we use dendritic polyaryl ether aminediacetic acid dendrimer (Gn-NA) as stabilizer for preparation of Gn-NA capped platinum nanoparticle (Pt@GnNAs). Pt@GnNAs showed nice stability and high activities in catalytic hydrogenation reactions for phenyl aldehydes.

## 2. Experimental

2.1. Chemicals

3,3-dihydroxybenzyl alcohol, 18-crown-6, benzyl bromide, and deuterated solvents were purchased from Acros Organics and used without further purification. The other solvents, carbon tetrabromide and H_2PtCl_6 were obtained from Shanghai Chemical Reagents Company.

2.2. Synthesis of polyaryl ether aminediacetic acid dendrons

The synthesis of G_2-NA was shown in Scheme 1. G_2-Br used for synthesis of G_2-NH_2 was prepared using Fréchet method [18]. G_2-NH_2 was synthesized according to an improved Gabriel method [19]. G_2-NH_2 (1.0 equiv.), methyl chloroacetate (2.1 equiv.) and anhydrous Na_2CO_3 (2.0 equiv.) mixed with 50 mL of DFM were heated at 90 °C for 36 h under magnetic stirring. The resultant mixture was cooled to room temperature and filtrated. The filtrate was concentrated to ca. 20 mL, and

* To whom correspondence should be addressed.
  E-mail: pyang@suda.edu.cn
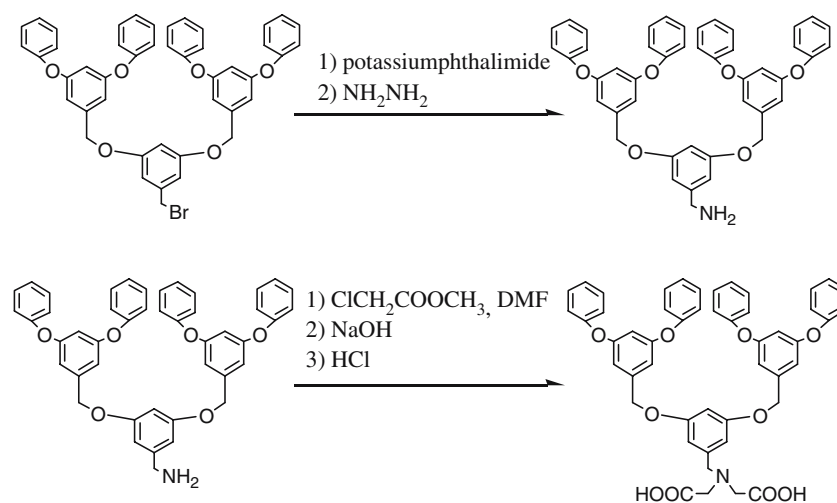
Scheme 1. Synthesis of G$_2$-NA.

then 50 mL of distilled water was added. The mixture was extracted with 100 mL portions of CH$_2$Cl$_2$. The solvent was removed on a rotary evaporator. The residue was mixed with aqueous solution of NaOH and refluxed for 5 h. The mixture was cooled to room temperature and neutralized with hydrochloric acid. A light yellow precipitate was formed. The mixture was filtered, washed with ethanol, and dried in a desiccator over calcium chloride to give light yellow solid product. The yield for G1-NA to G3-NA is around 50% ∼ 45%. The compounds were characterized by H^1 and C^{13} NMR, respectively.

2.3. Preparation of Gn-NA capped platinum nanoparticles (Pt@Gn-NA)

Polyaryl ether aminediacetic acid dendrons capped platinum nanoparticles were prepared using alcohol reduction method [20,21]. Briefly, 0.5 mmol of H$_2$PtCl$_6$ and proper amount of Gn-NA (the range of the molar ratio of H$_2$PtCl$_6$ and Gn-NA is between 1 and 60) were at first mixed in aqueous ethanol (100 mL). The solution was adjusted to pH 8∼ 9 under vigorous stirring at room temperature, and then was heated to reflux for 2 h resulting Pt@Gn-NA colloidal solution.

2.4. Hydrogenation reactions

Hydrogenation reactions were carried out in a 50 mL, three-necked round-bottomed Schlenk flask equipped with a hydrogen adapter, a dropping funnel, and a reflux condenser with a second adapter connected to a liquid paraffin bubbler. The system was purged with H$_2$ for 30 min before the reaction. Experiments were carried out by adding 10 mmol of substrate and ca. 0.011 mmol of catalyst dissolved in the EtOH–H$_2$O solvent system through the dropping funnel under vigorous stirring conditions. All of the hydrogenation reactions were carried out at atmospheric pressure.

2.5. Characterization

Transmission electron microscopy (TEM) studies were conducted on a TECNAI-12 electron microscope operating at 120 kV. Samples for TEM analysis were prepared by dropping one drop of diluted Pt@Gn-NA solution onto copper grids covered with Formvar, then dried in air and placed into the desiccator prior to measurement. X-ray-diffraction (XRD) patterns were obtained with a Philips diffractometer using Ni-filtered Cu Kα radiation. The samples were prepared as a thin film on a glass plate through evaporating the solvent of Pt@Gn-NA colloids. FTIR spectra were measured on a Nicolet Magna 550 spectrometer. UV-Vis absorption spectra of samples were recorded on TU1810 SPC spectrophotometer.

3. Results and discussion

At reflex temperature, the colour of the solution of G$_n$-NA dendrimer and H$_2$PtCl$_6$ did not change obviously in the first half hour, and then the colour of the solution changed from light yellow to dark brown in a few minutes. UV-visible spectra of the G$_2$-NA dendrimer-H$_2$PtCl$_6$ in aqueous ethanol solution during the reduction process are shown in Figure 1. The absorption band at 260 nm, which can be assigned to platinum ions, disappears after the reduction of H$_2$PtCl$_6$, indicating the formation of dendrimer capped platinum nanoparticles. A new band at around 310 nm can be attributed to the formation of acetaldehyde in the reduction process. After reduction the absorption intensity of the spectrum of the composite increases at low energy, this results from the interband transition of the encapsulated zero-valent metal particles [22].

Figure 2 shows a TEM image of Pt@G$_2$-NA (the molar ratio of H$_2$PtCl$_6$ and Gn-NA is 30) and the corresponding core-size histogram. It can be seen from the
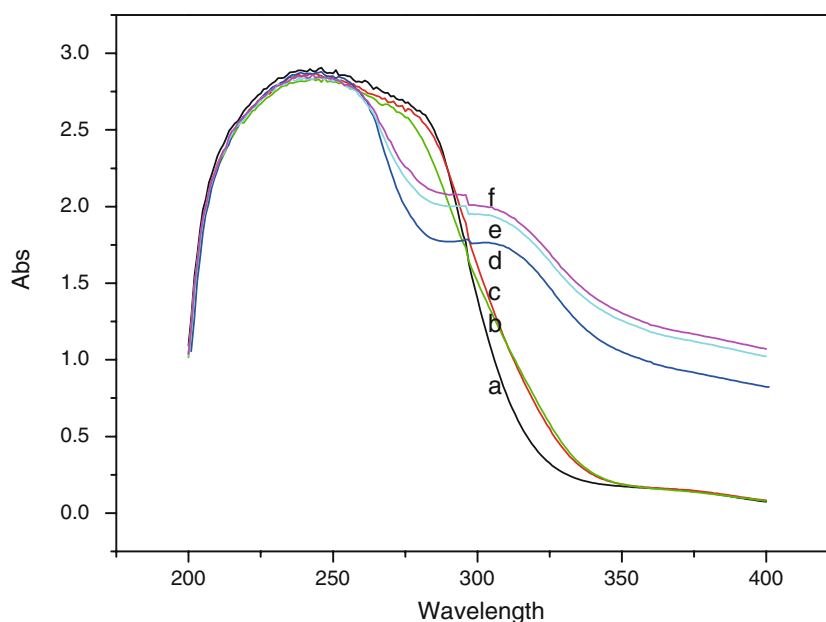
Figure 1. UV-visible spectra of H_2PtCl_6 and G_2-NA dendrimer in an aqueous ethanol solution during the reduction process. The molar ratio of Pt and G_2-NA is 30. Curves of a–f correspond to reflex the mixture 0, 10, 20, 30, 70 and 90 min.

figure that the platinum particles are small and the core sizes exhibit a relatively wide size distribution (1–3.5 nm). The average diameter and dispersivity obtained from the histogram plot are 2.4 ± 0.6 nm. The core diameter and the stability of the dendrimer capped Pt(0) nanoparticles depend on the molar ratio of metal/dendrimer. For Pt@G_2-NA, the average diameter of Pt(0) particles changed from 1.7 to 3.8 nm when the molar ratio of H_2PtCl_6/G_2-NA changed from 1 to 60. The dark brown solution of Pt@G_2-NA, in which the molar ratio of Pt/G_2-NA was less than 60, was stable without precipitation at room temperature for several weeks. However, black metal platinum precipitated from the colloidal solution in a few days when the molar ratio of Pt/G_2-NA was 100. Metal core size decreases when the dendrimer generation increases from one to two. The change of the dendrimer generation from two to three seems to have no obvious influence on the metal core size. The average particle size and the standard deviation of the Pt@G_n-NA particles are presented in Table 1. The formation of Gn-NA-stabilized platinum colloid can also be confirmed by XRD patterns of samples (Figure 3). The broadening of the peaks in the diffraction patterns demonstrated the small sizes of the colloidal particles.

Figure 4 shows the IR absorption spectrum of G_2-NA along with that of Pt@G_2-NA. The C=O stretching vibration of G_2-NA in salt form is at 1663 cm^{-1}, while the peak of C=O vibration of Pt@G_2-NA was at 1643 cm^{-1}. The peak shift to low wavenumber for Pt@G_2-NA was the evidence for the interaction between Pt cluster and carboxyl-terminated G_2-NA [23]. The dendrimer parts of the Pt@G_n-NA

consist mainly of aryl ether moieties. It is believed that the aryl ether moieties have no specific interaction with the metal core [14]. Thus, the dendrons are proposed to attach to the metallic core radially via Pt-carboxylate interactions. A G_2-NA capped platinum nanoparticle in an average diameter of 2.0 nm has around 280 Pt atoms in the metallic core. When the molar ratio of metal to dendrimer is 30, there are about nine G_2-NA dendrons attached to the metal core. Thus, the Pt@G_n-NA nanostructure can be described as that there are only a few G_n-NA dendrons attached on the surface of the platinum core via the interactions between the carboxyl groups of the dendrimer and surface Pt atoms of the metal nanoparticle. Most of the nanoparticle surface remains unpassivated. The interaction among two carboxyl groups terminated at the dendrimer and the metallic core is strong enough to keep the stability of the Pt@G_n-NA. Because of these properties, the Pt@Gn-NAs were supposed to be good metal catalysts for hydrogenations.

The composite catalysts used in this study are composed of Pt(0) nanoclusters capped with Gn-NA dendrimers, where dendrimer generation changes from one to three. Figure 5 shows representative successive UV-visible spectra of the hydrogenation of 3-phenoxybenzaldehyde catalyzed by Pt@G_2NA. The reduction process of 3-phenoxybenzaldehyde can be monitored by the disappearance of the 306 nm peak with the concomitant appearance of new absorption peaks at 265, 272 and 278 nm, which have been attributed to the ones of 3-phenoxybenzyl alcohol. The hydrogenation of other phenyl aldehydes can also be visualized by the disappearance of the absorption peak between 280 and

310 nm. The values of TOF are given in Table 2. The TOFs change from 91 to 25 depending on the dendrimer generation and substrates. The TOFs decrease for the same substrate catalyzed by Pt clusters capped with higher generations of the dendrimer. It seems that the Pt@Gn-NAs made from the first generation of dendrimer possess an open dendritic shell. The substrates easily access to the active sites through low generation of dendrimer with relative low steric hindrance and diffusion limitation. When the generation of the dendrimer increases, the greater steric bulk of the dendritic arms could limit accessibility of the substrates
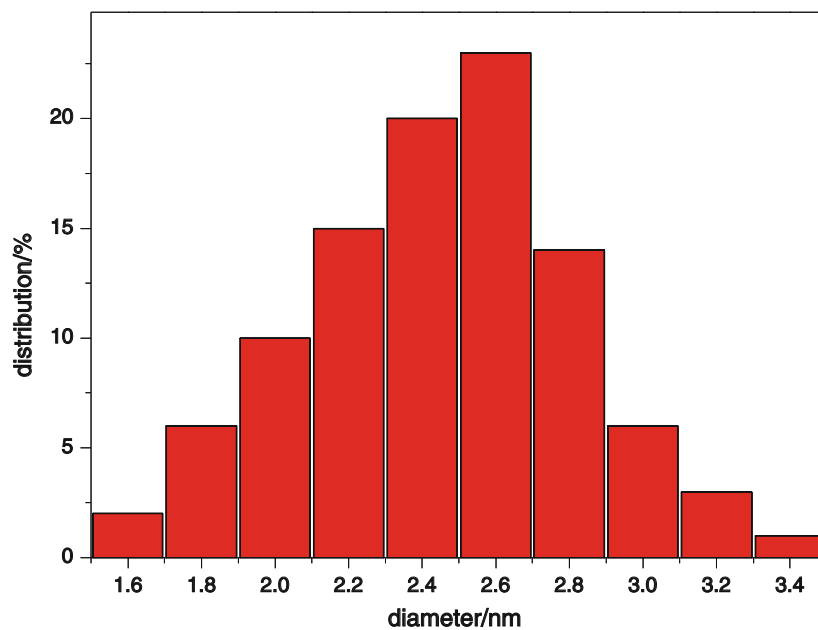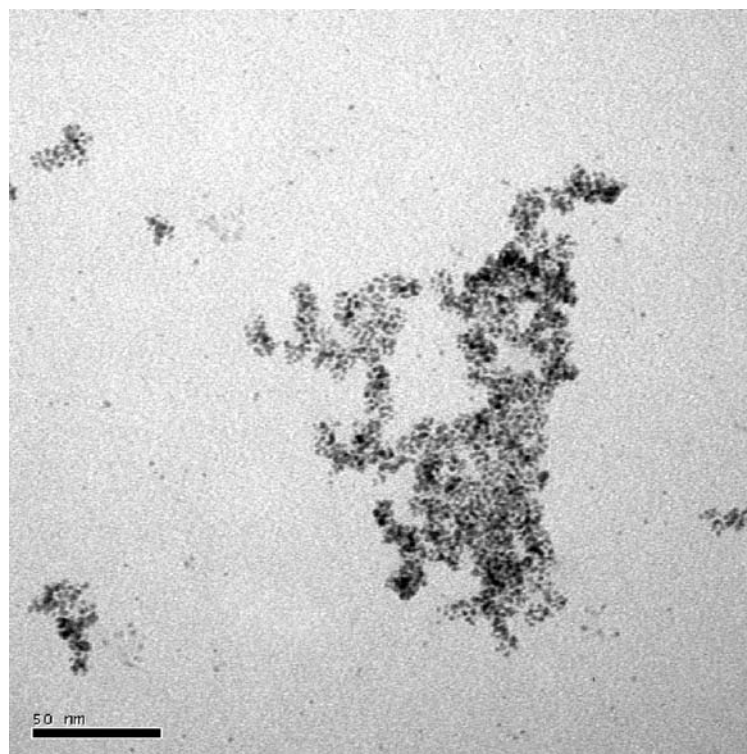
Figure 2. Transmission electron micrograph of Pt@G_2NA nanoparticles. The average size and standard deviation of the particles were ca 2.4 ± 0.58 nm. The molar ratio of Pt/G_2-NA was 30. The sample was prepared from an aqueous ethanol solution.

Table 1
Average particle size of Pt@G$_n$-NA

Mole ratio of Pt/G$_n$-NA	Particle size (nm)		
	Pt@G$_1$-NA	Pt@G$_2$-NA	Pt@G$_3$-NA
1	2.2 ± 0.50	1.7 ± 0.65	1.7 ± 0.58
30	3.4 ± 0.79	2.4 ± 0.58	2.4 ± 0.84
60	5.1 ± 1.38	3.8 ± 0.81	3.5 ± 0.71

to the active sites. With the most efficient catalyst that is the first generation dendrimer capped Pt nanoparticles, the 99% conversion of 3-phenoxybenzaldehyde is reached after ca. 25 h hydrogenation.

The catalytic activity of Pt@Gn-NA was influenced by the molar ratio of Pt and Gn-NA of the catalyst. Figure 6
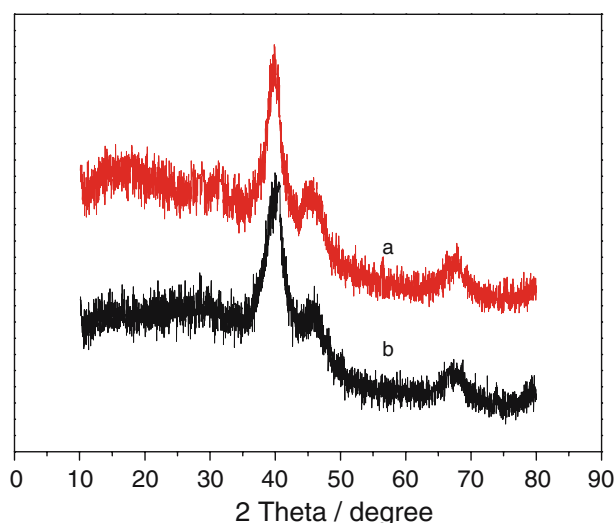
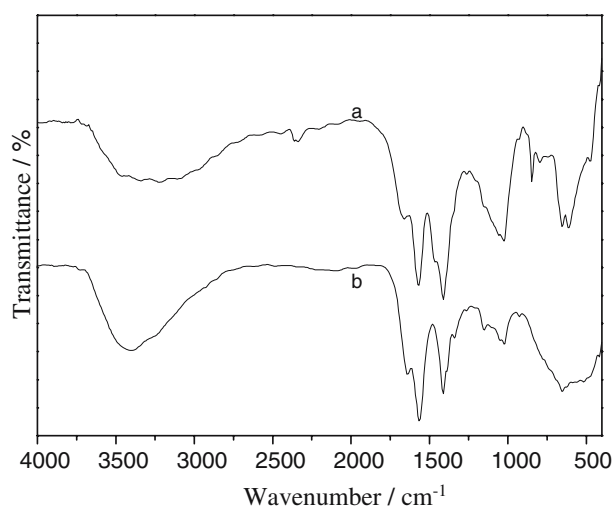Figure 3. XRD patterns of Pt@G$_2$NA (a), and Pt@G$_3$NA (b).

Figure 4. FTIR spectrum of G$_3$-NA (a) along with that of Pt@G$_3$-NA (b).

shows that the catalytic activity versus the composition of the catalyst. The TOFs of 3-phenoxybenzaldehyde hydrogenation increase as the molar ratio of Pt/G$_3$-NA increases from 1 to 20, then decrease as the molar ratio is beyond 20. The unprotected Pt suspension for 3-phenoxybenzaldehyde catalytic hydrogenation only shows low catalytic activity (TOF is ca. 28) under the same reaction conditions. These results show that the nanoparticles without protected by enough number of stabilizers will agglomerate in the reaction process, thus decreasing the catalytic activity.

For a particular catalyst, the TOFs generally decrease as the substrate having a substitutional group. The maximum TOF of the hydrogenation of phenyl aldehyde was 91 using Pt@G$_1$-NA as catalyst. A substrate having one phenoxy group at *meta*-position of phenyl aldehyde yielded a lower value of TOF. However, when the phenoxy group was changed to methoxyl group, the TOF decreased to 60. When a methoxyl group was present at the *para*-position of phenyl aldehyde, the TOF decreased further to 37. It seems that an electron donating group decreases activity of hydrogenation of phenyl aldehyde.

After a hydrogenation was completed, the Pt@G$_2$-NA catalyst was separated from the reaction mixture by evaporation the solvent and washed with EtOH, then dissolved in EtOH–H$_2$O solvent again. The spent Pt catalyst was used in the hydrogenation of 3-phenoxybenzaldehyde for three runs. The catalytic activity of Pt@G$_2$-NA for the hydrogenation was lost ca. 20% in the second run, and then the catalytic activity of Pt@G$_2$-NA was kept in the third run. However, the colour of dendritic Pt catalyst changed from dark brown to dark black throughout the reuse experiment. It should be mentioned that using dendritic polyaryl ether amine as a stabilizer can also get dendrimer capped Pt nanoparticles. However, black Pt precipitated in the
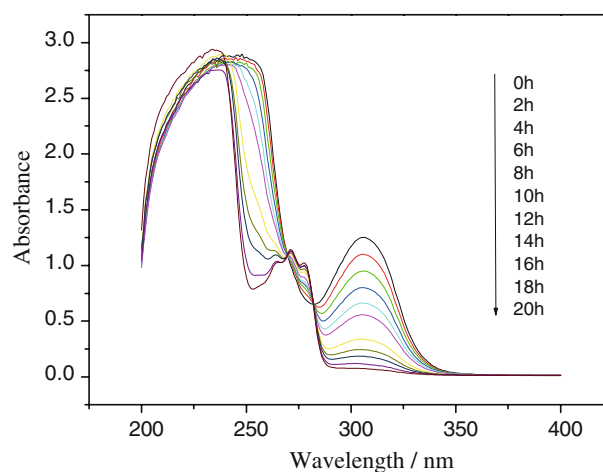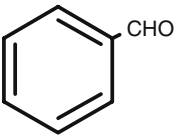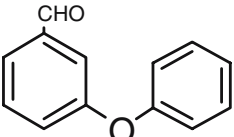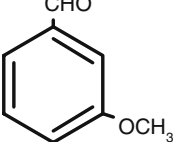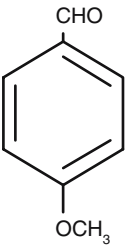

Figure 5. Successive UV-visible spectra of the hydrogenation of 3-phenoxybenzaldehyde catalyzed by Pt@G$_2$-NA. Reaction conditions: [Pt]:[G$_2$-NA] = 30; [substrate] : [Pt] = 900; Reaction temperature: 40 °C.

Table 2
Catalytic activity of Pt@G_n-NAs for hydrogenation of phenyl aldehydes

No	Substrate	λ_{max} (nm)	TOF/mol product per mol Pt per h		
			Pt@G1-NA	Pt@G2-NA	Pt@G3-NA
1		280	91	81	64
2		306	77	73	65
3		310	60	47	27
4		277	37	34	25

Molar ratio of Pt and Gn-NA: 30, Reaction temperature: 40 °C.

hydrogenation process. So we can conclude that using proper dendritic polyaryl ether aminediacetic acid as a stabilizer can get stable metal-nanoparticle and maintain the surface of the metal particle unpassivated for hydrogenation reactions.

4. Conclusions

Polyaryl ether aminediacetic acid dendrons capped Pt nanoparticles have been successfully prepared and the resulting nanoparticles effectively promote the
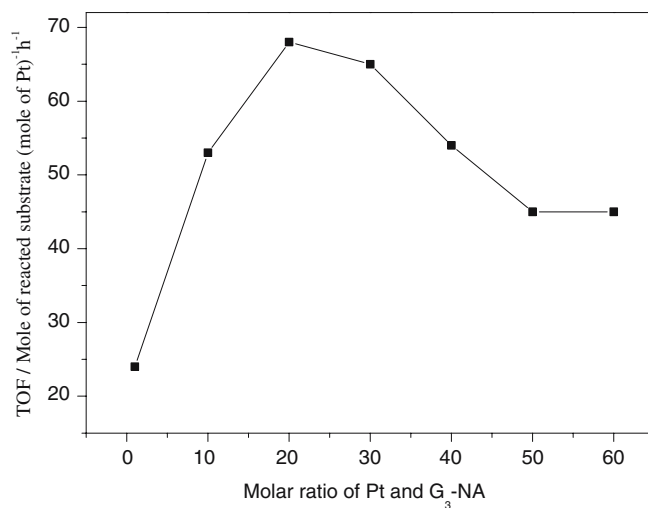

Figure 6. Dependence of TOFs of the hydrogenation of 3-phenoxybenzaldehyde on the molar ratio of Pt and G_3-NA. Reaction temperature: 40 °C.

hydrogenation of phenyl aldehydes. The Pt nanoparticles capped by the dendrimer shown high catalytic activity for the hydrogenation of phenyl aldehyde to phenyl alcohol under an atmospheric pressure of H_2. The Pt particles capped with Gn-NA are stable during the catalytic hydrogenation process and can be easily recovered and reused. The result suggests the effectiveness of dendritic polyaryl ether aminediacetic acid as a stabilizer for the preparation of Pt nanoparticle catalysts.

Acknowledgements

References

[1] D.L. Feldheim and C.A. Foss Jr., (eds), Metal nanoparticles: synthesis, characterization and applications, (Marcel Dekker: New York, 2002).

[2] G. Schmidt(.), *Clusters and Colloids* (VCH, Weinheim, 1994).

[3] R.M. Crooks, M.Q. Zhao, L. Sun, V. Chechik and L.K. Yeung, Acc. Chem. Res. 34 (2001) 181.

[4] D. Astruc and F. Chardac, Chem. Rev. 101 (2001) 2991–3023.

[5] M.Q. Zhao and R.M. Crooks, J. Am. Chem. Soc. 120 (1998) 4877–4878.

[6] L. Balogh and D.A. Tomalia, J. Am. Chem. Soc. 120 (1998) 7355–7356.

[7] F. Gröhn, B.J. Bauer, Y.A. Akpalu, C.L. Jackson and E.J. Amis, Macromolecules 33 (2000) 6042–6050.

[8] K.R. Gopidas, J.K. Whitesell and M.A. Fox, J. Am. Chem. Soc. 125 (2003) 6491.

[9] O.M. Wilson, R.W.J. Scott, J.C. Garcia-Martinez and R.M. Crooks, J. Am. Chem. Soc. 127 (2005) 1015–1024.

[10] M. Zhao and R.M. Crooks, Angew. Chem. Int. Ed. 38 (1999) 364–366.

[11] Y.H. Niu, L.K. Yeung and R.M. Crooks, J. Am. Chem. Soc. 123 (2001) 6840–6846.

[12] R.W.J. Scott, O.M. Wilson and R.M. Crooks, J. Phys. Chem. B 109 (2005) 692–704.

[13] E.H. Rahim, F.S. Kamounah, J. Frederiksen and J.B. Christensen, Nano Lett. 1 (2001) 499–501.

[14] K.R. Gopidas, J.K. Whitesell and M.A. Fox, Nano Lett. 3 (2003) 1757–1760.

[15] K. Esumi, R. Isono and T. Yoshimura, Langmuir 20 (2004) 237–243.

[16] Y.-M. Chung and H.-K. Rhee, Catal. Lett. 85 (2003) 159–164.

[17] M. Ooe, M. Murata, T. Mizugaki, K. Ebitani and K. Kaneda, Nano Lett. 2 (2002) 999–1002.

[18] C.J. Hawker and J.M.J. Fréchet, J. Am. Chem. Soc. 112 (1990) 7638.

[19] J.C. Sheehan and W.A. Bolhofer, J. Am. Chem. Soc. 72 (1950) 2786.

[20] J.H. Youk, J. Locklin, C. Xia, M.K. Park and R. Advincula, Langmuir 17 (2001) 4681.

[21] H. Hirai, Y. Nakao and N. Toshima, J. Macromol. Sci. Chem. A 13 (1979) 727.

[22] G. Schmid, *Cluster and Colloids: From Theory to Applications* (VCH, New York, 1994).

[23] J. Petroski and M.A. El-Sayed, J. Phys. Chem. A 107 (2003) 8371–8375.